



# Halide anion-templated assembly of di- and triiodoperfluorobenzenes into 2D and 3D supramolecular networks

Gabriella Cavallo<sup>a</sup>, Serena Biella<sup>a,b</sup>, Jian Lü<sup>a</sup>, Pierangelo Metrangolo<sup>a,b,\*</sup>, Tullio Pilati<sup>c</sup>, Giuseppe Resnati<sup>a,b,c,\*\*</sup>, Giancarlo Terraneo<sup>a,b</sup>

<sup>a</sup> NFMLab - D.C.M.I.C. "Giulio Natta", Politecnico di Milano, Via L. Mancinelli 7, 20131 Milan, Italy

<sup>b</sup> CNST - IIT@POLIMI, Politecnico di Milano, Via G. Pascoli 70/3, 20133 Milan, Italy

<sup>c</sup> C.N.R. - I.S.T.M., University of Milan, Via C. Golgi 19, 20133 Milan, Italy

## ARTICLE INFO

### Article history:

Received 4 April 2010

Received in revised form 13 May 2010

Accepted 13 May 2010

Available online 11 June 2010

### Keywords:

Fluorobenzene

Halide anions

Halogen bonding

Self-assembly

Crystal engineering

Supramolecular chemistry

Dedicated to Professor Russell

P. Hughes on the occasion of receiving the 2010 ACS Award for Creative Work in Fluorine Chemistry.

## ABSTRACT

The single crystal structures of five co-crystals formed by the reaction of different iodide and bromide salts with di- and triiodoperfluorobenzenes (I-ArF) are reported. All of these perfluorocarbon-hydrocarbon systems are heteromeric three-component systems, wherein the weakly coordinating cations favour the formation of naked halides, which function as electron-donors towards the I-ArF modules. The analysis of the crystal structures shows that  $I^- \cdots I-ArF$ , and  $Br^- \cdots I-ArF$  halogen bonds (XBs) control the self-assembly of the obtained supramolecular architectures. 2D and 3D supramolecular networks have been obtained, wherein naked iodide and bromide anions act as tri-, tetra-, or pentadentate nodes. The selected examples demonstrate that I-ArF modules can be particularly robust and reliable tectons for XB-based coordination of halide ions and afford supramolecular architectures in a rational and predictable way.

© 2010 Elsevier B.V. All rights reserved.

## 1. Introduction

Interactions involving halogen atoms as electrophilic species (Lewis acid) have been named halogen bonding (XB) [1] to highlight the similarities they share with the hydrogen bonding (HB) in which an electropositive hydrogen atom functions as electron-acceptor. In fact, the electron density distribution around monovalent chlorine, bromine, and iodine atoms is highly anisotropic and an electropositive region ( $\sigma$ -hole) frequently exists on the extension of the covalent bond [2]. This electropositive crown is surrounded by an electroneutral ring and, further out, an electronegative belt. Halogen atoms can thus work as electron-donors in directions perpendicular to the covalent bond (at the electronegative belt) and as electron-

acceptors on the extension of the covalent bond (at the electropositive crown). XB is a strong and specific interaction and, as a consequence of the anisotropic distribution of the electron density around halogen atoms, also directional enough to be particularly effective in geometry-based design and supramolecular construction. Molecular iodine is known to function as an effective electrophilic species (XB-donor) since mid-nineteen century and a large variety of molecular complexes involving iodine have been obtained on its self-assembly with electron-donors (Lewis bases) [3]. However, the variety of electron-donors which can be paired with iodine is limited by its low reduction potential. Moreover, while with weak electron-donors iodine functions as a bidentate electron-acceptor, with stronger Lewis bases (e.g. some nitrogen heterocycles) the polarization of the  $I_2$  molecule is increased to the point that interaction occurs at only one of the iodine atoms [4]. This electron density transfer from one iodine to the other may even result in amphoteric behaviour of  $I_2$  molecules, with the second iodine atom serving as a Lewis base towards another  $I_2$  molecule and forming neutral polyiodine systems [5].

Organic polyiodides are less prone than  $I_2$  to oxidize sensitive donors and they are also more robust and predictable than  $I_2$  in the

\* Corresponding author at: Dipartimento di Chimica, Materiali ed Ingegneria Chimica "Giulio Natta", Politecnico di Milano, Via L. Mancinelli 7, 20131 Milan, Italy. Tel.: +39 02 2399 3041; fax: +39 02 2399 3180.

\*\* Corresponding author at: NFMLab - D.C.M.I.C. "Giulio Natta", Politecnico di Milano, Via L. Mancinelli 7, 20131 Milan, Italy. Tel.: +39 02 2399 3032.

E-mail addresses: [pierangelo.metrangolo@polimi.it](mailto:pierangelo.metrangolo@polimi.it) (P. Metrangolo), [giuseppe.resnati@polimi.it](mailto:giuseppe.resnati@polimi.it) (G. Resnati).

pattern of XB they inherently tend to form. The carbon chain significantly attenuates the effect that the XB formation at one iodine atom has on the binding profile of the other iodine(s) atom(s) [6]. For instance, telechelic organic diiodides function as bidentate XB-donors whenever possible.

The extent of the electropositive crown on the extension of the covalent bond increases with the polarizability of the halogen and with the electron withdrawing power of the neighbouring groups on the carbon skeleton [7]. Fluorination of a halocarbon is thus a powerful strategy to boost its XB-donor capability. For example, the positive charge on the iodine atom of iodomethane derivatives is 0.009 in CH<sub>3</sub>I and 0.165 in CF<sub>3</sub>I [8]. Thanks to the electron-withdrawing ability of fluorine atoms, aliphatic or aromatic iodoperfluorocarbons, and to a lesser extent their bromo analogues, are particularly robust tectons in XB based supramolecular chemistry [9]. In the past decade, numerous papers describing supramolecular architectures formed by haloperfluoroalkanes and -arenes with neutral electron-donors have drawn attention to the ability of these halocarbons to function as versatile building blocks in crystal engineering [10].

As far as the XB-acceptor partner is concerned, an increased electron density on the electron-donor site increases its Lewis basicity thus promoting its involvement in the formation of strong and directional XB. As a consequence, anions are better XB-acceptors than neutral species, therefore XB can be expected to have a great potential in the coordination and binding of anionic species [11]. Anion coordination chemistry is receiving increasing attention due to the fundamental roles anions play in many chemical and biological processes [12]. Moreover, anionic species like phosphate and nitrate from agricultural fertilisers and pertechnetate from nuclear implants can have deleterious effects as pollutants in the environment. Anion binding and recognition are thus major issues from both the fundamental and applicative points of view and research in the field is very active [13].

HB has been the noncovalent interaction by far most frequently employed for the design of anion receptors [14], but ionic bonds with positively charged receptors (like polyammonium [15], guanidinium, and imidazolium cations [16]) or coordination to metal ions [17] have also been used. Anions, particularly halides, participate readily as XB-acceptors in the solid state [18] and recently XB-based anion coordination and templation is proving a useful complement to the opportunities given by other interactions [19]. The design and synthesis of the first receptors based on multidentate XB-donors are appearing [20] and useful applications have also been reported [19d].

In this paper we will describe the formation of five halogen-bonded supramolecular networks. They are the perfluorocarbon-hydrocarbon co-crystals **3–5**, **8**, and **9** and they have been obtained on self-assembly of iodide and bromide salts (namely the cryptated derivatives **1a,b** and the ammonium derivatives **6a,b**) with 1,4-diiodotetrafluorobenzene (**2**) and 1,3,5-trifluoro-2,4,6-triiodobenzene (**7**). We already reported that when **2** self-assembles with tetra-*n*-butylammonium chloride or bromide, both the iodobenzene derivative and the halide anion function as bidentate modules. 1D halogen-bonded copolymers are formed wherein the donor and acceptor modules alternate [21]. Examples reported in this paper show that the self-assembly of two- or threefold symmetry XB-donors with naked halide anions form halogen-bonded 2D and 3D supramolecular networks. Clearly iodofluoroarenes are robust tectons in XB-driven anion coordination and templation and easily form 1D, 2D, and 3D haloperfluorocarbon supramolecular anions. Up to five XBs were found to occur around the same iodide anion thus providing further insight into the design of multidentate XB-donor receptor molecules capable of tight binding of anionic species via the cooperative action of multiple XBs.

## 2. Results and discussion

The number of XBs formed by a given anion is a key issue in halogen-bonded driven anion binding as it contributes to identify the anion coordination number. Similar to cations, for which the number of coordinated ligands is usually greater than the cation charge, anions have a “primary valence” that is the negative charge of the anion and a “secondary valence” provided by the noncovalent interactions they give rise to on interaction with the Lewis acids forming the anion coordination sphere [22]. In most cases these acids are HB-donors as the presence of strong or weak HB-donor sites (e.g. O–H or C–H residues, respectively) is ubiquitous in organic compounds. The formation of a halogen-bonded adduct involving anions can be interpreted as a XB-donor substituting for a HB-donor in the coordination sphere of the anion. Such substitution may occur at one, or some, or all of the sites available in the coordination sphere of the anion. This accounts for the variability of the number of XBs formed by a given anion.

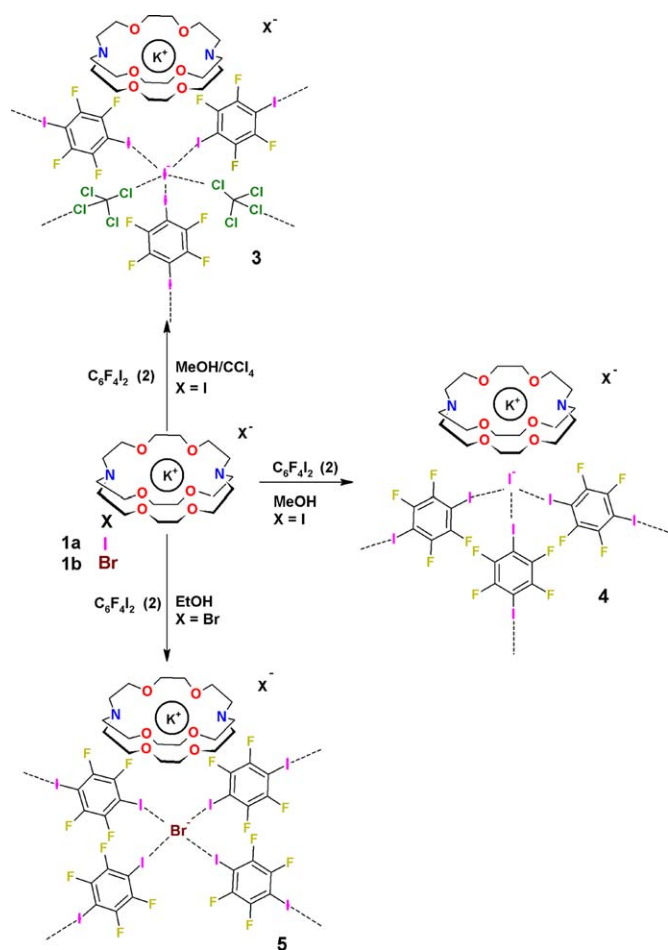
The chemical composition of the system, the geometry of the interacting moieties, and the overall requirements of the crystal packing can strongly affect the coordination sphere of the involved anion, and hence the number of XBs it can give rise to. We have already observed that halide ions have a moderate bias towards the formation of two or three XBs [23]. However, a careful crystal engineering can induce them to form up to eight halogen bonds [24]. Clearly, the more naked a given anion is, the higher its tendency to function as XB-acceptor and the greater the number of XBs it gives rise to. It is thus not surprising that anions paired with weakly coordinating cations are more prone to form a particularly high number of XBs.

In general, halogen-bonded supramolecular architectures formed by anions can be divided into two groups, *heteromeric two-component systems* and *heteromeric three-component systems* [11c]. This classification helps a lot in the identification of the key-factors determining the number of XBs a given anion is involved in. In *heteromeric two-component systems* a halogenated organic cation functions as the XB-donor moiety and the anion functions as the XB-acceptor one. In this kind of systems the necessity to balance positive and negative charges in the crystal heavily affects the number of XBs formed by the anion as the number of C–X moieties present in the halocarbon cation frequently becomes the limiting factor for the number of XBs given by the anion. In *heteromeric three-component systems* the anion is the XB-acceptor, the cation plays virtually no active role, as far as XB is concerned, and the XB-donor is a third neutral component that is present in the crystal. In these systems, there is no other limiting factor in the number, geometry, and topology of XBs but the ability of the anions to template the XB-donor partner(s). As a consequence, these three-component systems are better tailored to study the XB potential in anion coordination chemistry than the two-component systems. Here we describe five cases of halogen-bonded *heteromeric three-component systems*.

### 2.1. Co-crystals **3**, **4**, and **5**

Perfluorocarbon-hydrocarbon co-crystals **3** and **4** were prepared starting from the tetrafluoro-diiodobenzene **2**, as the XB-donor module, and the cryptate K<sub>2</sub>.2.2.2.⊂KI **1a**, as the XB-acceptor module. The co-crystal **5** has been similarly obtained on self-assembly of **2** with the cryptate K<sub>2</sub>.2.2.2.⊂KBr **1b** (Scheme 1).

Single crystals of **3** were grown under isothermal conditions (*T* = 298 K) by using the diffusion technique with a methanol/tetrachloromethane system. The melting point of **3** (491–497 K) is sharp thus indicating that it is a new well-defined chemical species rather than a mechanical mixture of the two starting modules.



Single crystal X-ray diffraction analysis revealed that **3** crystallizes in the  $P-1$  space group and that **1a** and **2** are present in a 2:3 ratio. In fact, iodide ions are tridentate XB-acceptors and bind three different iodine atoms belonging to three distinct

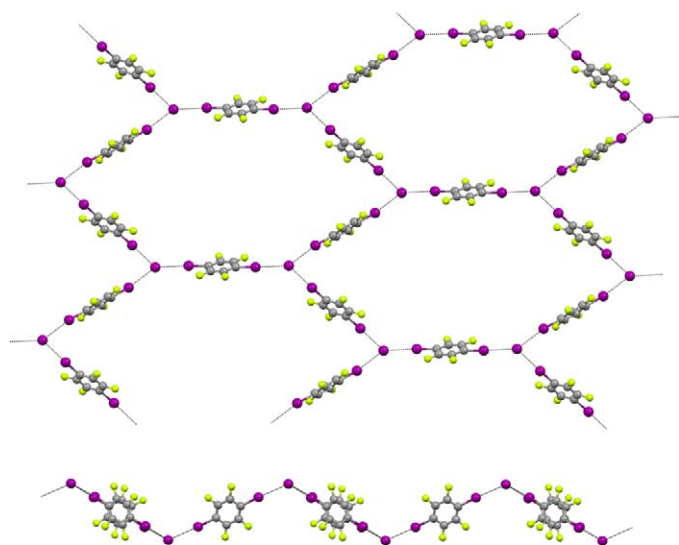


**Fig. 1.** Anionic supramolecular network of **3** sustained by  $I \cdots I$  interactions. Two projections of the 2D honeycomb-like sheets. XBs are dotted lines. Colour code: Grey, carbon; yellowish green, fluorine; violet, iodine. (For interpretation of the references to colour in this figure legend, the reader is referred to the web version of the article.)

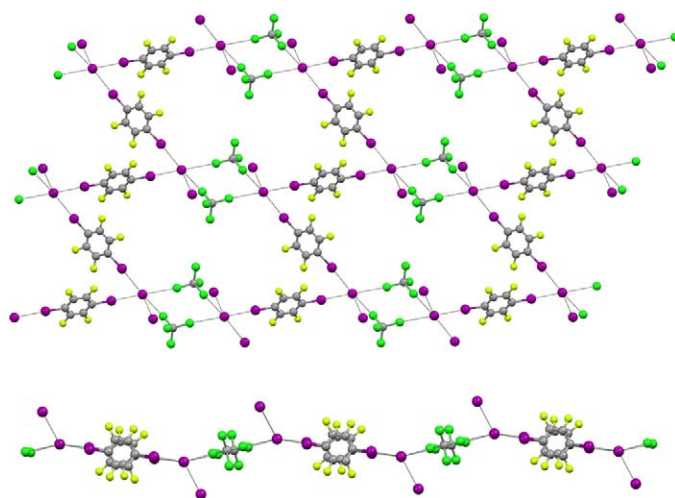


**Fig. 2.** Anionic supramolecular network of **3** sustained by  $I \cdots I$  and  $I \cdots Cl$  interactions: Two projections of the 2D honeycomb-like sheet. XBs are dotted lines. Colour code: Green chlorine; other colours as in Fig. 1. (For interpretation of the references to colour in this figure legend, the reader is referred to the web version of the article.)

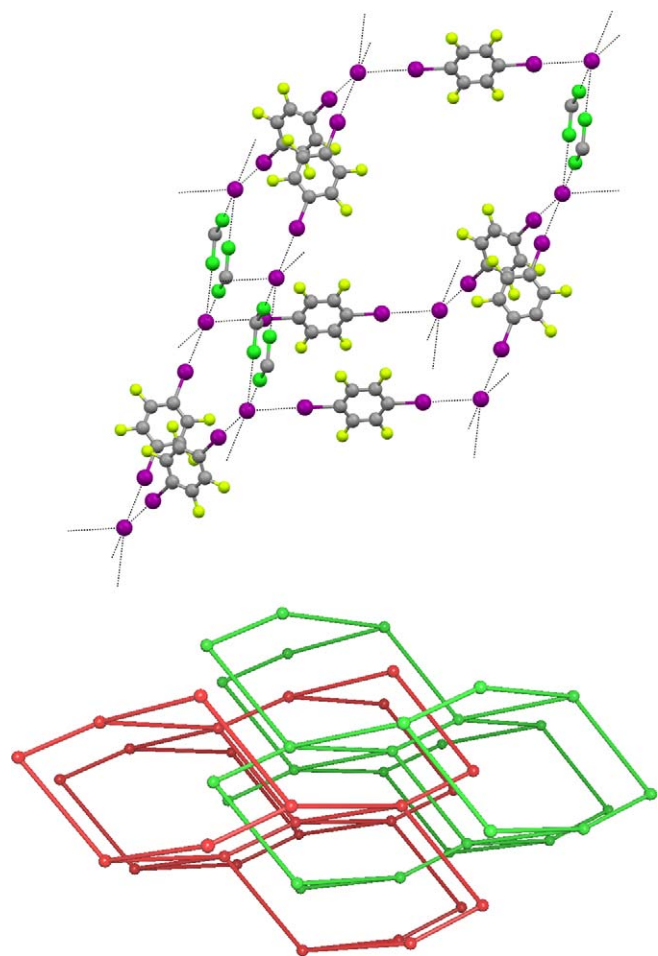


**Fig. 3.** Top: A single adamantanoid 3D unit of the anionic supramolecular network identified in **3** if all  $I \cdots I$  and  $I \cdots Cl$  interactions are considered. XBs are dotted lines. Colour codes as in Fig. 2. Bottom: Two interpenetrated adamantanoid networks of the XB-based 3D lattice are plotted in red and green with the software Topos 4.0 [26]. (For interpretation of the references to colour in this figure legend, the reader is referred to the web version of the article.)

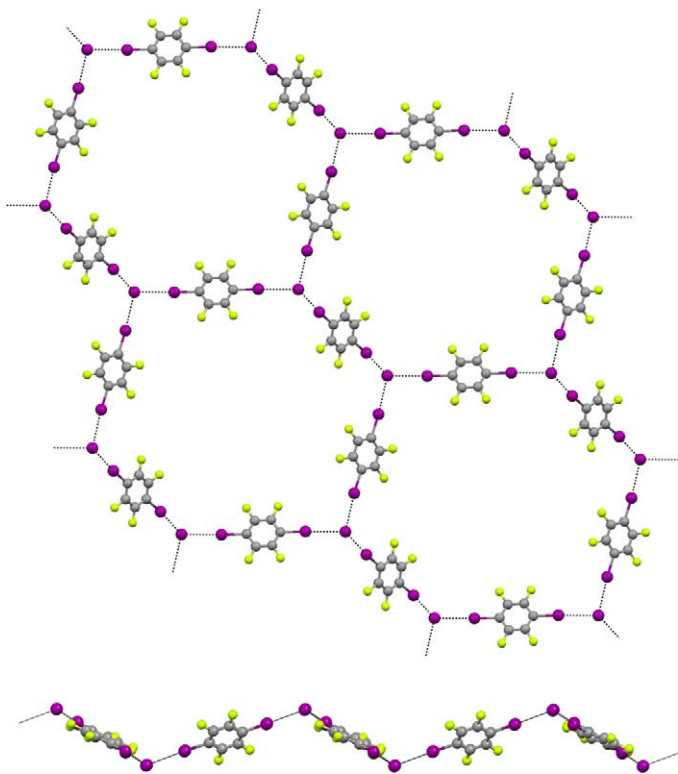


**Fig. 4.** Anionic supramolecular network of **4** sustained by  $I^- \cdots I$  interactions. Two projections of the 2D honeycomb-like sheets. XBs are dotted lines. Colour codes as in Fig. 1. (For interpretation of the references to colour in this figure legend, the reader is referred to the web version of the article.)

tetrafluorobenzene molecules, which, in turn, function as bidentate and telechelic XB-donors. This connectivity around the iodine atoms translates into infinite and highly undulated 2D honeycomb-like sheets parallel to each other and topologically equivalent to (6,3) networks (Fig. 1). Each distorted hexagon is defined by six  $I^-$  ions (vertexes) and six molecules of **2** (sides); the six  $I^-$  ions are non-coplanar as the hexagon adopts approximately a chair-like conformation. The  $I \cdots I$  contacts in **3**, span the range 3.435–3.442 Å and the  $I \cdots I \cdots I$  angles are 72.33°, 112.60°, and 123.68°.

As a measure of the strength of XB, we define ‘normalized contact’ as the ratio  $Nc = D_{ij}/(rvdwi + rvdwj)$ , where  $D_{ij}$  is the distance between the atoms  $i$  and  $j$  and  $rvdwi$  and  $rvdwj$  are the corresponding van der Waals radii or Pauling radii for atoms or anions, respectively [25].  $Nc$  is a useful indicator of the interaction strength, better than the distance  $D_{ij}$  itself, because it allows us to compare distances between couple of atoms or anions of different nature. For the XBs in the undulated 2D honeycomb-like sheets of **3**,  $Nc$  is about 0.83.

Parallel sheets are then linked together by  $I^- \cdots Cl-C$  XBs. In fact, two molecules of carbon tetrachloride bridge two  $I^-$  ions belonging to two parallel sheets thanks to twofold  $I^- \cdots Cl-CCl_2-Cl \cdots I^-$  interactions. Chlorocarbons are usually worse XB-donors than iodocarbons and it is no surprise that  $I^- \cdots Cl$  distances span the range 3.521–3.587 Å, that corresponds to  $Nc = 0.90$ –0.92. The overall result is that in this co-crystal each iodide ion is pentadentate, namely it participates in the formation of five different halogen bonds, which are organized around the  $I^-$  ion in a distorted pyramidal geometry having the rectangular base made by two iodine and two chlorine atoms, while the apex, quite asymmetrically placed with respect to the base, is the third iodine. If the connectivities of both the  $I^- \cdots I$  and the  $I^- \cdots Cl$  XBs are taken into account and if the two tetrachloromethane molecules bridging iodide ions are considered, from a topological point of view, a single

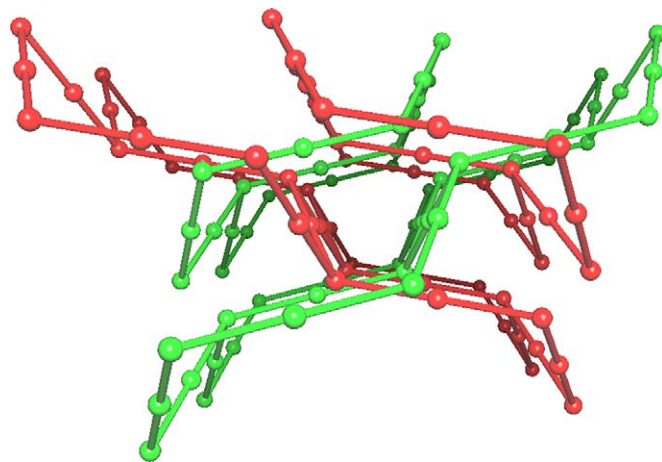


**Fig. 5.** Interpenetration mode in the 3D structure of the co-crystal **4** prepared by slow and isothermal ( $T = 298$  K) evaporation of an ethanol solution of the cryptate  $K_2.2.2.CrKI$  **1a**, as the source of naked halide anions, and 1,4-diiodotetrafluorobenzene **2** as the XB-donor module. Cations have been omitted for clarity.

bridge between the ions, a new 2D hexagonal network can be identified in the structure of **3** where the vertexes of the large and distorted hexagons are six  $I^-$  anions and the sides are four molecules of **2** and two pairs of  $CCl_4$  molecules (Fig. 2). Once again the six  $I^-$  ions

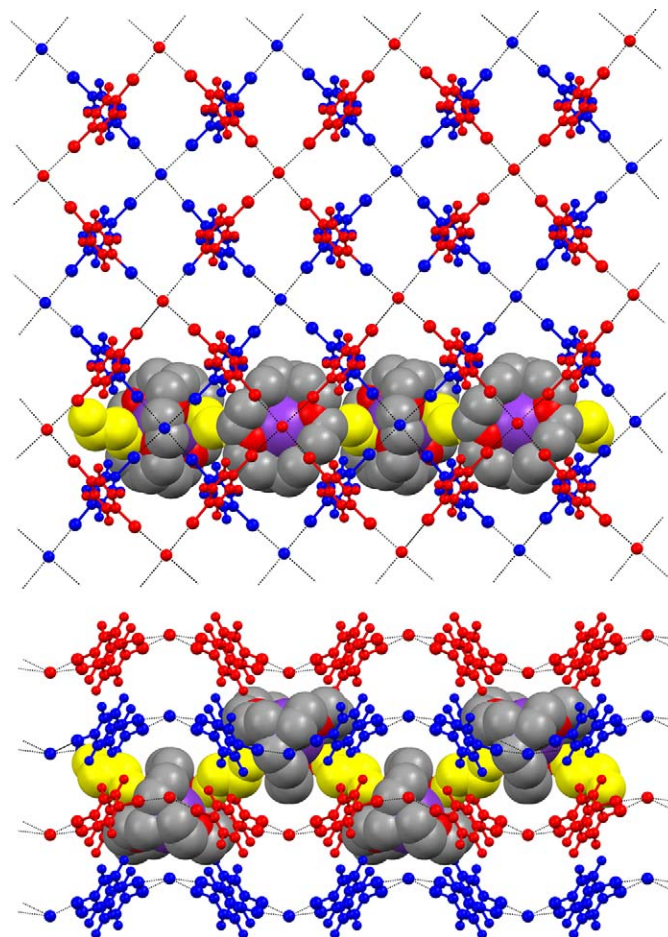
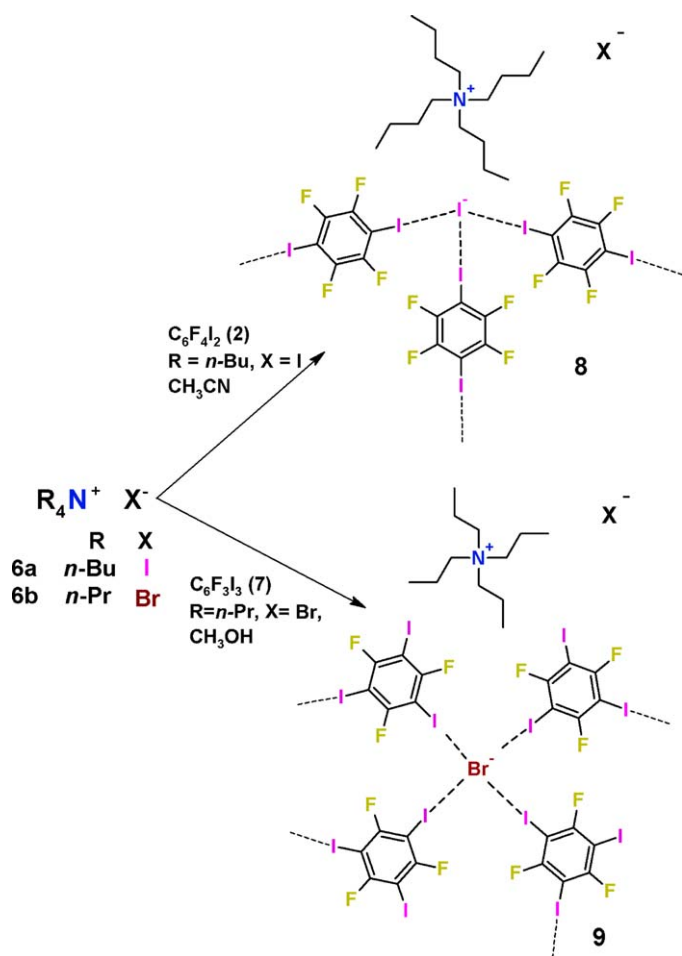


**Fig. 6.** Co-crystal **5** obtained on self-assembly of **1b** and **2**. XBs are dotted lines. *Top:* Projection perpendicular to the sheets; two adjacent layers are plotted (in red and blue) to show clearly the squared (4,4) structure. *Bottom:* Four (4,4) layers of **5** and a chain of cations (in grey) bonded through HB by ethanol molecules (in yellow). Nearest layers are plotted with different colours (red and blue). (For interpretation of the references to colour in this figure legend, the reader is referred to the web version of the article.)



**Scheme 2.** Co-crystals **8** and **9** prepared on self-assembly of ammonium salts **6a,b** with XB-donors **2** and **7**, for **8** and **9**, respectively.

are not coplanar and the hexagon adopts approximately a chair-like conformation. The overall connectivity of the two hexagonal networks (presented separately in Figs. 1 and 2) gives rise to a 3D diamond network ( $6^6\text{-dia}$ ) with twofold interpenetration along  $[1,0,0]$  with full interpenetration vectors (class Ia) (Fig. 3) [26].

Interestingly, if the self-assembly reaction of **1a** with **2** is carried out in pure methanol, the co-crystal **4** is obtained where, no  $CCl_4$  being available, iodide ions are tridentate, rather than pentadentate as in **3**. In fact, X-ray diffraction analysis of **4** revealed that, consistent with the robust and predictable tricoordination pattern of XBs preferred by iodide anions, the iodide salt **1a** and the diiodotetrafluorobenzene module **2** are present in a 2:3 ratio and  $I^- \cdots I^- \cdots I^-$  XBs form 2D (6,3) honeycomb-like sheets similar to those seen in **3** (Fig. 4). These sheets are much more regular than in **3** as the  $I^- \cdots I^- \cdots I^-$  angles are closer to the tetrahedral geometry ( $101.65^\circ$ ,  $107.62^\circ$ , and  $119.45^\circ$ ). As the electron density of iodide anions is now distributed over three XBs, the  $I^- \cdots I^-$  contacts are shorter, namely stronger, than in **3** ( $3.352\text{--}3.379$  Å,  $Nc \approx 0.81$ ). In the 3D structure of **4**, the 2D (6,3) layers are arranged in two sets of parallel layers oriented along the  $[1, -1, 1]$  and  $[1, 1, 1]$  directions and catenated with each other in a parallel-parallel (p-p) arrangement (Fig. 5). A 2D  $\rightarrow$  3D inclined polycatenated structure [27] is formed and the dihedral angle of the inclined layers is  $62.7^\circ$ . The structural difference between **3** and **4** also reflects in their melting point difference, in fact, co-crystal **4** melts in the range  $467\text{--}471$  K, almost  $20^\circ$  lower than co-crystal **3**.

Self-assembly of  $K_2.2.2.\text{C}KBr$  **1b** and diiodotetrafluorobenzene **2** afforded single crystals amenable to X-ray analysis from ethanol

solution. The obtained solid **5** shows a melting point lower than **3** and **4** ( $369\text{--}371$  K) and contains the bromide salt **1b** and the diiodotetrafluorobenzene **2** in a 2:1 ratio. A disordered ethanol molecule simulating glycerol and bonded to the cation by HB is also present. As expected, the  $Br^- \cdots I^-$  XBs are responsible for the self-assembly of two starting building blocks, but the compositional differences between the bromide co-crystals **5** and iodide analogues **3** and **4** produce tremendous topological changes. In fact, in **5** bromide anions function as tetradentate XB-acceptors yielding 2D (4,4) grid structure (Fig. 6).  $Br^-$  ions sit at the nodes of a slightly distorted square and bridge four different diiodotetrafluorobenzene molecules, which, in turn, function as bidentate and telechelic XB-donors. Each square is thus defined by four  $Br^-$  ions (vertexes) and four molecules of **2** (sides). The  $Br^- \cdots I^-$  contacts in **5** span the range  $3.280\text{--}3.350$  Å ( $Nc$  is  $0.82\text{--}0.84$ ) and the  $I^- \cdots Br^- \cdots I^-$  angles are almost right angles, spanning the range  $85.53\text{--}90.97^\circ$ . Since the XB-pattern around the bromide anions is not perfectly planar, slightly undulated 2D sheets are obtained. The cations sit perfectly in the centre of the formed square frame so that interpenetration is prevented. Two parallel sheets, translated along the diagonal of the square, bring two  $Br^-$  anions on the top and at the bottom of the cations which are thus surrounded by six  $Br^-$  anions arranged according to a distorted octahedron.

## 2.2. Co-crystals **8** and **9**

Co-crystals **8** and **9** were prepared using organic ammonium salts as a source of naked halide anions. Single crystals of **8** were obtained from acetonitrile solution by slow isothermal ( $T = 298$  K) evaporation of the solvent starting from tetra-*n*-butyl ammonium iodide (**6a**) as source of  $I^-$  anions and 1,4-diiodotetrafluorobenzene (**2**) as the XB-donor (Scheme 2). Also in this case, the melting point

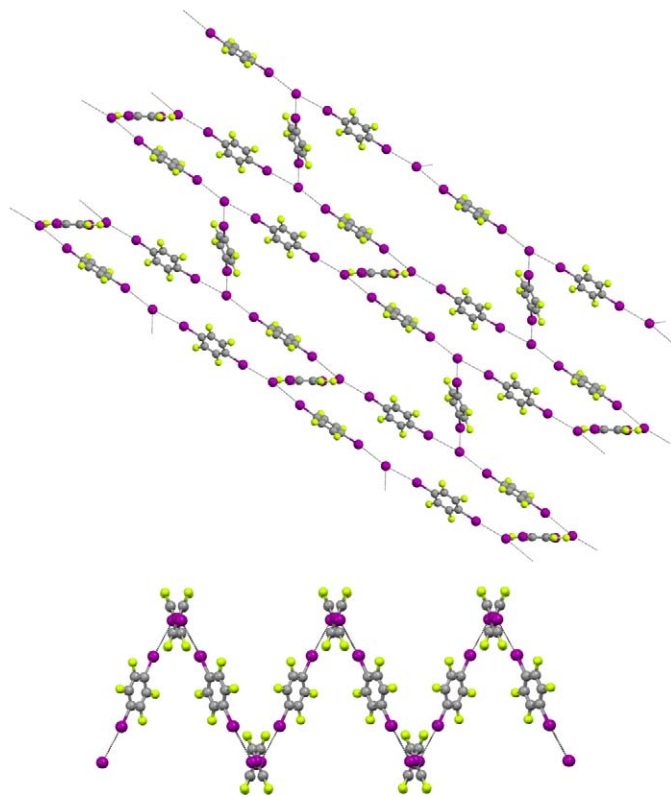


**Fig. 7.** A (6,3) layer of the anionic supramolecular network of **8** seen on top of and parallel to the wrinkle. XBs are dotted lines. Colour codes as in Fig. 1. (For interpretation of the references to colour in this figure legend, the reader is referred to the web version of the article.)

analysis gave a clear indication that **8** is a new well-defined chemical species rather than a mechanical mixture of the starting modules, with sharp melting at 413–418 K, versus 418–421 K and 393 K for **6a** and **2**, respectively.

Single crystal X-ray analysis of **8** revealed that the diiodotetrafluorobenzene **2** and the iodide salt **6a** are present in a 3:2 ratio. Similar to **3** and **4**, iodide anions are halogen-bonded to three different iodine atoms belonging to three distinct diiodotetrafluorobenzenes, which, in turn, function as bidentate and telechelic XB-donors. The I···I···I angles are 169.95°, 116.56°, and 69.38° and the connectivity around the iodide anions forms highly corrugated (6,3) networks which appear as folded sheets, the folding angle being about 53° (Fig. 7). The I···I contacts span the range 3.481–3.658 Å with  $N_c = 0.84$ –0.88.

The co-crystal **9** was prepared by slow isothermal ( $T = 298$  K) evaporation of a methanol solution containing tetra-*n*-propyl ammonium bromide (**6b**) as a source of Br<sup>−</sup> anions and 1,3,5-trifluoro-2,4,6-triiodobenzene (**7**) as the XB-donor. The sharp melting point of co-crystal **9** (495–499 K) is clearly different from the ones of the starting compounds (**6a**: 539–545 K; **7**: 431–432 K)

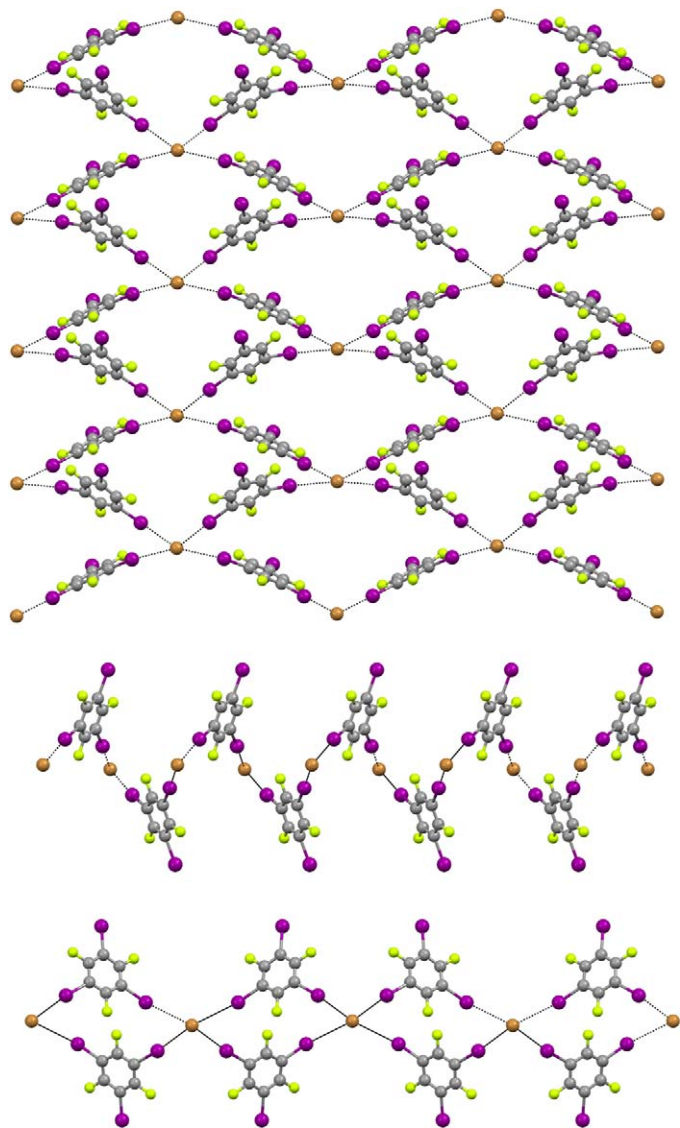


**Fig. 8.** Three orthogonal projections of the (4,4) layer of the anionic supramolecular network of **9**. XBs are dotted lines. Colour code: brown, bromine; other colours as in Fig. 1. (For interpretation of the references to colour in this figure legend, the reader is referred to the web version of the article.)

indicating the formation of a new well-defined chemical species. Single crystal X-ray analysis revealed that in the co-crystal **9** the starting triiodotrifluorobenzene module **7** and the ammonium salt are present in a 2:1 ratio. As far as the XB is concerned, the bromide anion functions as a tetradentate XB-acceptor bridging four different modules **7**, while **7** in its turn gives rise to two halogen bonds with two bromide ions. As a consequence of this XB-based connectivity, a 2D highly corrugated (4,4) grid structure is formed (Fig. 8), wherein Br<sup>−</sup> ions sit at the nodes of a highly distorted square defined by four Br<sup>−</sup> ions (vertexes) and four molecules of **7** (sides). The Br<sup>−</sup>···I contact lengths are 3.291 Å and 3.562 Å, corresponding to  $N_c = 0.83$  and 0.89. The I···Br···I angles are very far from to be right angles, spanning the range 70.74–124.47°. For each square, two adjacent aromatic rings are oriented so that the third iodine atom (not involved in Br<sup>−</sup>···I contacts) points upwards, while in the other two aromatic rings the third iodine atom points downwards, as it is clearly shown in the projection at the bottom of Fig. 8. These iodine atoms not involved in Br<sup>−</sup>···I contacts are involved in short contacts with fluorine atoms belonging to aromatic rings in the two adjacent grids (I···F distance is 3.248 Å,  $N_c = 0.94$ ). Clearly, the stronger Br<sup>−</sup>···I XBs are the force driving the formation of the (4,4)-network, while the weaker I···F interactions link contiguous sheets.

### 3. Conclusions

In this paper we have described the synthesis and single crystal X-ray structures of five perfluorocarbon-hydrocarbon co-crystals where the architectures of the formed supramolecular networks are mainly controlled by I···I–ArF, and Br<sup>−</sup>···I–ArF XBs. Three of the described assemblies contain iodide anions as XB-acceptors, while bromide anions are present in the remaining two structures. All of the obtained co-crystals are heteromeric three-component systems, wherein the cation is a weakly coordinating species (either a cryptate complex of **1a,b** or a tetraalkylammonium cation of **6a,b**) thus favouring the formation of naked halide anions in solution. These naked anions function as very strong electron-donors towards the electron poor iodine atoms of 1,4-diiodotetrafluorobenzene (**2**) and 1,3,5-trifluoro-2,4,6-triiodobenzene (**7**), which in turn are very good XB-donor molecules thanks to the fluorination of the aromatic rings.

The 2D structures of these co-crystals suggest iodide and bromide anions have some preferential patterns of XBs. In general, halides have a moderate bias towards the formation of two or three XBs [11c–21]. Results reported in this paper suggest that this bias may be stronger for iodide anions than for bromide anions. In fact, bromide accepts four XBs both in co-crystals **5** and **9** and 2D (4,4) nets are present in both structures (Figs. 6 and 8). Three I···I XBs are present both in **3** and **4** and **8**, the three co-crystals all showing 2D (6,3) nets (Figs. 1, 4 and 7). The CCl<sub>4</sub> solvent used for the synthesis of **3** offers further opportunities of XB formation to the strong XB-acceptor ability of I<sup>−</sup> anions which thus behave as pentadentate XB-acceptors which give rise to three I···I XBs (involving diiodotetrafluorobenzene) and to two I···Cl XBs (involving tetrachloromethane). The hexagonal frameworks present in **3**, **4**, and **8**, are then forced to interpenetration in co-crystal **3** and **4** or to wrinkle in **8** in order to satisfy the close packing requirements.

The co-crystals detailed in this paper demonstrate that diiodo- and triiodoperfluorobenzenes can be particularly robust and reliable tectons for XB-based coordination of halides. Anion coordination and anion-templated assembly processes under the control of XB are still in their infancy but they are expected to have a bright future. New tectons in anion coordination chemistry allow new families of supramolecular synthons to be involved in self-assembly and self-organization processes. As a result, new

materials with unprecedented characteristics and functional properties are expected [6].

## 4. Experimental

### 4.1. General

Commercial HPLC-grade solvents were used without further purification. Starting materials were purchased from Sigma–Aldrich, Acros Organics, and Apollo Scientific. Reactions were carried out in oven-dried glassware under a nitrogen atmosphere. Melting points were determined with a Reichert instrument by observing the melting and crystallizing processes through an optical microscope. Thermal analyses were recorded with a Linkam DSC600 Stage (temperature range:  $-196$  to  $+600$  °C) coupled with a LN94 cooling system. FT-IR spectra were obtained in KBr pellets with a Perkin Elmer 2000 FT-IR spectrometer. The units for wave numbers were  $\text{cm}^{-1}$  and values rounded to  $1 \text{ cm}^{-1}$  upon automatic assignment. The X-ray crystal structures were determined using a Bruker Smart Apex diffractometer.

### 4.2. Synthesis of K.2.2.2. $\cdot$ KI and K.2.2.2. $\cdot$ KBr 1

Equimolar amount of 4,7,13,16,21,24-hexaoxa-1,10-diazabicyclo[8,8,8]hexacosane (K.2.2.2.) and KI or KBr were dissolved respectively in ethyl acetate and MeOH. The two solutions were mixed and heated to reflux. After 1 h, the solvent was evaporated and white microcrystalline powders were obtained.

K.2.2.2. $\cdot$ KI (**1a**): m.p.: 553 K; FT-IR:  $\nu_{\text{max}}$  (selected bands): 2964; 2862; 2816; 1478; 1434; 1360; 1298; 1260; 1099; 1027; 935; 827; 756.

K.2.2.2. $\cdot$ KBr (**1b**): m.p.: 533–539 K; FT-IR:  $\nu_{\text{max}}$  (selected bands): 2965; 2872; 2812; 2753; 1476; 1432; 1356; 1290; 1256; 1091; 1081; 1028; 942; 931; 829; 740.

### 4.3. Co-crystallization experiments

In a typical co-crystallization procedure, equimolar amounts of the XB-donor and acceptor were separately dissolved at room temperature in the right solvent as reported in Table 1, using just the amount of solvent necessary for complete dissolution. The slow evaporation technique under isothermal conditions ( $T = 298 \text{ K}$ ) was used to obtain co-crystals **4**, **5**, **8** and **9**; the saturated solutions containing both the XB-donor and acceptor were mixed in a clear borosilicate glass vial which was left open in a closed cylindrical wide-mouth bottle containing paraffin oil. Solvents were allowed to slowly evaporate at room temperature and to be absorbed by paraffin oil until crystals were formed in a period ranging 3–5 days.

Co-crystal **3** was obtained adopting the diffusion technique. Thus after mixing the two solutions containing the XB-donor and acceptor, the clear borosilicate glass vial was placed open in a closed cylindrical wide-mouth bottle containing  $\text{CCl}_4$ . Solvents were allowed to mix by slow diffusion from the gas to the liquid

phase under isothermal conditions ( $T = 298 \text{ K}$ ) until crystals were formed in 3 days.

All the obtained crystals were filtered off the mother liquor, washed gently with *n*-pentane and rapidly dried in air at room temperature.

Co-crystal **3** m.p.: 491–497 K; FT-IR:  $\nu_{\text{max}}$  (selected bands): 2961; 2882; 1450; 1361; 1297; 1259; 1209; 1101; 1079; 948; 932; 831; 748.

Co-crystal **4** m.p.: 467–471 K; FT-IR:  $\nu_{\text{max}}$  (selected bands).

Co-crystal **5** m.p.: 369–371 K; FT-IR:  $\nu_{\text{max}}$  (selected bands): 2883; 2816; 1454; 1442; 1350; 1295; 1259; 1213; 1132; 1103; 1076; 1027; 951; 938; 835; 754.

Co-crystal **8** m.p.: 413–418 K; FT-IR:  $\nu_{\text{max}}$  (selected bands): 2959; 2871; 1455; 1437; 1382; 1363; 1210; 939; 876; 755.

Co-crystal **9** m.p.: 495–499 K; FT-IR:  $\nu_{\text{max}}$  (selected bands): 2970; 2879; 1558; 1471; 1453; 1395; 1327; 1036; 981; 967; 753; 708.

Crystallographic data for co-crystals **3–5**, **8** and **9** can be obtained free of charge from the Cambridge Crystallographic Data Centre via [www.ccdc.cam.ac.uk/data\\_request/cif](http://www.ccdc.cam.ac.uk/data_request/cif) under reference numbers CCDC 771886–771890, respectively.

Summary of data CCDC 771886 (**3**)

Formula:  $\text{C}_{28} \text{H}_{36} \text{Cl}_4 \text{F}_6 \text{I}_4 \text{K}_1 \text{N}_2 \text{O}_6$

Unit cell parameters:  $a$  10.1750(12),  $b$  10.8919(12),  $c$  20.123(3),  $\alpha$  100.04(2),  $\beta$  93.82(2),  $\gamma$  92.40(2)

Space group  $P-1$

Summary of data CCDC 771887 (**4**)

Formula:  $\text{C}_{27} \text{H}_{36} \text{F}_6 \text{I}_4 \text{K}_1 \text{N}_2 \text{O}_6$

Unit cell parameters:  $a$  13.454(2),  $b$  16.965(2),  $c$  16.825(2),  $\beta$  91.86(2)

Space group  $P21/n$

Summary of data CCDC 771888 (**5**)

Formula:  $\text{C}_{32} \text{H}_{42} \text{Br}_1 \text{F}_8 \text{I}_4 \text{K}_1 \text{N}_2 \text{O}_7$

Unit cell parameters:  $a$  19.508(2),  $b$  12.2682(12),  $c$  18.076(2)

Space group  $Pbcn$

Summary of data CCDC 771889 (**8**)

Formula:  $\text{C}_{25} \text{H}_{36} \text{F}_6 \text{I}_4 \text{N}_1$

Unit cell parameters:  $a$  9.5925(15),  $b$  13.064(2),  $c$  25.491(5),  $\beta$  94.95(2)

Space group  $P21/n$

Summary of data CCDC 771890 (**9**)

Formula:  $\text{C}_{24} \text{H}_{28} \text{Br}_1 \text{F}_6 \text{I}_6 \text{N}_1$

Unit cell parameters:  $a$  17.689(2),  $b$  21.888(3),  $c$  9.1721(12)

Space group  $Pnma$

## Acknowledgments

The financial support from Fondazione Cariplo (Project “New-Generation Fluorinated Materials as Smart Reporter Agents in  $^{19}\text{F}$  MRI”) and MIUR (Project “Engineering of the Self-assembly of Molecular Functional Materials via Fluorous Interactions”) are gratefully acknowledged.

## References

- [1] (a) P. Metrangolo, G. Resnati, *Science* 321 (2008) 918–919; (b) A. Farina, S.V. Meille, M.T. Messina, P. Metrangolo, G. Resnati, *Angew. Chem.*

**Table 1**

Experimental crystallization techniques used for the obtainment of co-crystals **3–5**, **8** and **9**.

Co-crystals	XB-acceptor	XB-donor	Solvent	Crystallization technique
<b>3</b>	K.2.2.2. $\cdot$ KI	$\text{C}_6\text{F}_4\text{I}_2$	$\text{MeOH}/\text{CCl}_4$	Diffusion
<b>4</b>	K.2.2.2. $\cdot$ KI	$\text{C}_6\text{F}_4\text{I}_2$	MeOH	Slow evaporation
<b>5</b>	K.2.2.2. $\cdot$ KBr	$\text{C}_6\text{F}_4\text{I}_2$	EtOH	Slow evaporation
<b>8</b>	$\text{NBu}_4\text{I}$	$\text{C}_6\text{F}_4\text{I}_2$	$\text{CH}_3\text{CN}$	Slow evaporation
<b>9</b>	$\text{NPr}_4\text{Br}$	$\text{C}_6\text{F}_3\text{I}_3$	MeOH	Slow evaporation

- Int. Ed. 38 (1999) 2433–2436;
- (c) E. Corradi, S.V. Meille, M.T. Messina, P. Metrangolo, G. Resnati, *Tetrahedron Lett.* 40 (1999) 7519–7523;
- (d) E. Corradi, S.V. Meille, M.T. Messina, P. Metrangolo, G. Resnati, *Angew. Chem., Int. Ed.* 39 (2000) 1782–1786;
- (e) A. Lunghi, P. Cardillo, M.T. Messina, P. Metrangolo, G. Resnati, *J. Fluor. Chem.* 91 (1998) 191–194;
- (f) M.T. Messina, P. Metrangolo, W. Panzeri, E. Ragg, G. Resnati, *Tetrahedron Lett.* 39 (1998) 9069–9072;
- (g) P. Metrangolo, H. Neukirch, T. Pilati, G. Resnati, *Acc. Chem. Res.* 38 (2005) 386–395;
- (h) A. Karpfen, in: P. Metrangolo, G. Resnati (Eds.), *Halogen Bonding Fundamentals and Applications*, Springer, Berlin, 2008, pp. 1–16.
- [2] (a) F.F. Awwadi, R.D. Willet, K.A. Peterson, B. Twamley, *Chem. Eur. J.* 12 (2006) 8952–8960;
- (b) P. Politzer, P. Lane, M.C. Concha, Y. Ma, J.S. Murray, *J. Mol. Model.* 13 (2007) 305–311;
- (c) P. Auffinger, F.A. Hays, E. Westhof, P.S. Ho, *Proc. Natl. Acad. Sci. U.S.A.* 101 (2004) 16789–16794;
- (d) J.S. Murray, M.C. Concha, P. Lane, P. Hobza, P. Politzer, *J. Mol. Model.* 14 (2008) 699–704;
- (e) P. Politzer, J.S. Murray, M.C. Concha, *J. Mol. Model.* 14 (2008) 659–665;
- (f) T. Brinck, J.S. Murray, P. Politzer, *Int. J. Quant. Chem.: Quant. Biol. Symp.* 19 (1992) 57–64.
- [3] (a) F. Guthrie, *J. Chem. Soc.* 16 (1863) 239–244;
- (b) D.S. Reddy, D.C. Craig, A.D. Rae, G.R. Desiraju, *J. Chem. Soc., Chem. Commun.* 23 (1993) 1737–1739.
- [4] R.D. Bailey, G.W. Drake, M. Grabarczyk, T.W. Hanks, L.L. Hook, W.T. Pennington, *J. Chem. Soc., Perkin Trans. 2* (1997) 2773–2779.
- [5] E.L. Rimmer, R.D. Bailey, T.W. Hanks, W.T. Pennington, *Chem. Eur. J.* 6 (2000) 4071–4081.
- [6] P. Metrangolo, F. Meyer, T. Pilati, G. Resnati, G. Terraneo, *Angew. Chem., Int. Ed.* 47 (2008) 6114–6127.
- [7] T. Clark, M. Hennemann, J.S. Murray, P. Politzer, *J. Mol. Model.* 13 (2007) 291–296.
- [8] (a) G. Valerio, G. Raos, S.V. Meille, P. Metrangolo, G. Resnati, *J. Phys. Chem. A* 104 (2000) 1617–1620;
- (b) R. Bianchi, A. Forni, T. Pilati, *Chem. Eur. J.* 9 (2003) 1631–1638.
- [9] (a) P. Metrangolo, G. Resnati, T. Pilati, S. Biella, in: P. Metrangolo, G. Resnati (Eds.), *Halogen Bonding Fundamentals and Applications*, Springer, Berlin, 2008, pp. 105–136;
- (b) P. Metrangolo, G. Resnati, *Chem. Eur. J.* 7 (2001) 2511–2519;
- (c) R.G. Gonnade, M.S. Shashidhar, M.M. Bhadbhade, *J. Indian Inst. Sci.* 87 (2007) 149–165.
- [10] (a) H.L. Nguyen, P.N. Horton, M.B. Hursthouse, A.C. Legon, D.W. Bruce, *J. Am. Chem. Soc.* 126 (2004) 16–17;
- (b) P. Metrangolo, C. Präsang, G. Resnati, R. Liantonio, A.C. Whitwood, D.W. Bruce, *Chem. Commun.* (2006) 3290–3292;
- (c) V. Mugnaini, C. Punta, R. Liantonio, P. Metrangolo, F. Recupero, G. Resnati, G.F. Pedullì, M. Lucarini, *Tetrahedron Lett.* 47 (2006) 3265–3269;
- (d) K. Boubekeur, J.L. Syssa-Magalé, P. Palvadeau, B. Schöllhorn, *Tetrahedron Lett.* 47 (2006) 1249–1252;
- (e) E. Cariati, A. Forni, S. Biella, P. Metrangolo, F. Meyer, G. Resnati, S. Righetto, E. Tordin, R. Ugo, *Chem. Commun.* (2007) 2590–2592;
- (f) R. Liantonio, P. Metrangolo, T. Pilati, G. Resnati, A. Stevenazzi, *Cryst. Growth Des.* 3 (2003) 799–803;
- (g) D.B. Fox, R. Liantonio, P. Metrangolo, T. Pilati, G. Resnati, *J. Fluor. Chem.* 125 (2004) 271–281;
- (h) P. Metrangolo, W. Panzeri, F. Recupero, G. Resnati, *J. Fluor. Chem.* 114 (2002) 27–33.
- [11] (a) D.W. Bruce, P. Metrangolo, F. Meyer, C. Präsang, G. Resnati, G. Terraneo, A.C. Whitwood, *New J. Chem.* 32 (2008) 477–482;
- (b) G. Gattuso, R. Liantonio, P. Metrangolo, F. Meyer, G. Resnati, A. Pappalardo, M.F. Parisi, T. Pilati, I. Pisagatti, G. Resnati, *Supramol. Chem.* 18 (2006) 235–246;
- (c) P. Metrangolo, T. Pilati, G. Terraneo, S. Biella, G. Resnati, *CrystEngComm* 11 (2009) 1187–1196.
- [12] (a) A. Bianchi, K. Bowman-James, E. García-Españaed, *Supramolecular Chemistry of Anions*, Wiley–VCH, New York, 1997;
- (b) J.L. Sessler, P.A. Gale, W.S. Cho, *Anion Receptor Chemistry*, Royal Society of Chemistry, Cambridge, UK, 2006.
- [13] (a) P.A. Gale, *Coord. Chem. Rev. Special Issue: 35 Years of Synthetic Anion Receptor Chemistry, 1968–2003* 240 (2003) 1–226;
- (b) P.A. Gale, *Coord. Chem. Rev. Special Issue: Anion Coordination Chemistry II* 250 (2006) 2917–3244.
- [14] (a) P. Anzenbacher Jr., R. Nishiyabu, M.A. Palacios, *Coord. Chem. Rev.* 250 (2006) 2929–2938;
- (b) J.L. Sessler, J.M. Davis, *Acc. Chem. Res.* 34 (2001) 989–997;
- (c) T.K. Chandrashekar, S. Venkatraman, *Acc. Chem. Res.* 36 (2003) 676–691;
- (d) R. Misra, T.K. Chandrashekar, *Acc. Chem. Res.* 41 (2008) 265–279;
- (e) A.P. Davis, *Coord. Chem. Rev.* 250 (2006) 2939–2951;
- (f) M.H. Filby, J.W. Steed, *Coord. Chem. Rev.* 250 (2006) 3200–3218;
- (g) M.D. Lankshear, P.D. Beer, *Acc. Chem. Res.* 40 (2007) 657–668;
- (h) V. Amendola, D. Esteban-Gomez, L. Fabbrizzi, M. Licchelli, *Acc. Chem. Res.* 39 (2006) 343–353;
- (i) P.A. Gale, *Acc. Chem. Res.* 39 (2006) 465–475.
- [15] (a) E. García-Españaed, P. Díaz, J.M. Llinares, A. Bianchi, *Coord. Chem. Rev.* 250 (2006) 2952–2986;
- (b) K. Wichmann, B. Antonoli, T. Söhnel, M. Wenzel, K. Gloe, K. Gloe, J.R. Price, L.F. Lindoy, A.J. Blake, M. Schröder, *Coord. Chem. Rev.* 250 (2006) 2987–3003.
- [16] (a) E.A. Katayev, Y.A. Ustynyuk, J.L. Sessler, *Coord. Chem. Rev.* 250 (2006) 3004–3037;
- (b) C. Schmuck, *Coord. Chem. Rev.* 250 (2006) 3053–3067.
- [17] E.J. O’Neil, B.D. Smith, *Coord. Chem. Rev.* 250 (2006) 3068–3080.
- [18] (a) G. Minguez Espallargas, L. Brammer, J. van de Streek, K. Shankland, A.J. Florence, H. Adams, *J. Am. Chem. Soc.* 128 (2006) 9584–9585;
- (b) A. Casnati, G. Cavallo, P. Metrangolo, G. Resnati, F. Uguzzoli, R. Ungaro, *Chem. Eur. J.* 15 (2009) 7903–7912.
- [19] (a) R. Liantonio, P. Metrangolo, T. Pilati, G. Resnati, *Cryst. Growth Des.* 3 (2003) 355–361;
- (b) R. Liantonio, P. Metrangolo, F. Meyer, T. Pilati, W. Navarrini, G. Resnati, *Chem. Commun.* (2006) 1819–1820;
- (c) S.V. Lindeman, J. Hecht, J.K. Kochi, *J. Am. Chem. Soc.* 125 (2003) 11597–11606;
- (d) P. Metrangolo, F. Meyer, T. Pilati, G. Resnati, G. Terraneo, *Chem. Commun.* (2008) 1635–1637;
- (e) P. Metrangolo, Y. Carcenac, M. Lahtinen, T. Pilati, K. Rissanen, A. Vij, G. Resnati, *Science* 323 (2009) 1461–1464.
- [20] (a) A. Mele, P. Metrangolo, H. Neukirch, T. Pilati, G. Resnati, *J. Am. Chem. Soc.* 127 (2005) 14972–14973;
- (b) M.G. Sarwar, B. Dragisic, S. Sagoo, M.S. Taylor, *Angew. Chem.* 122 (2010) 1718–1721.
- [21] A. Abate, S. Biella, G. Cavallo, F. Meyer, H. Neukirch, P. Metrangolo, T. Pilati, G. Resnati, G. Terraneo, *J. Fluor. Chem.* 130 (2009) 1171–1177.
- [22] J. Kristin Bowman, *Acc. Chem. Res.* 38 (2005) 671–678.
- [23] (a) H. Bock, S. Holl, *Z. Naturforsch. B: Chem. Sci.* 56 (2001) 152–163;
- (b) A. Casnati, R. Liantonio, P. Metrangolo, G. Resnati, R. Ungaro, F. Uguzzoli, *Angew. Chem., Int. Ed.* 45 (2006) 1915–1918.
- [24] (a) G. Gattuso, A. Pappalardo, M.F. Parisi, I. Pisagatti, F. Crea, R. Liantonio, P. Metrangolo, W. Navarrini, G. Resnati, T. Pilati, S. Pappalardo, *Tetrahedron* 63 (2007) 4951–4958;
- (b) M. Ghassemzadeh, K. Harms, K. Dehnicke, *Chem. Ber.* 129 (1996) 115–120;
- (c) H. Bock, S. Holl, *Z. Naturforsch. B: Chem. Sci.* 57 (2002) 843–858;
- (d) H.M. Yamamoto, J.I. Yamaura, R. Kato, *J. Am. Chem. Soc.* 120 (1998) 5905–5913;
- (e) S.V. Rosokha, I.S. Neretin, T.Y. Rosokha, J. Hecht, J.K. Kochi, *Heteroatom Chem.* 17 (2006) 449–459;
- (f) T. Nakamoto, Q. Wang, Y. Miyazaki, M. Sorai, *Polyhedron* 21 (2002) 1299–1304.
- [25] A. Bondi, *J. Phys. Chem.* 68 (1964) 441–451.
- [26] All the formed networks in co-crystals **3–5**, **8**, and **9** were analyzed with the software Topos 4.0 by V.A. Blatov, *IUCr CompComm. Newsletter* 2006, 7, 4; see also <http://www.topos.ssu.samara.ru>.
- [27] For a tutorial on interpenetration modes, please have a look at <http://www.chem.monash.edu.au/staff/sbatten/interpen/index.html>.